The Pyrolysis of 3-Picoline: Ab Initio Quantum Chemical and Experimental (Shock Tube) Kinetic Studies

JEFFREY JONES, GEORGE B. BACSKAY, AND JOHN C. MACKIE*
School of Chemistry, University of Sydney, NSW 2006, Australia

(Received 15 December 1995 and in revised form 12 March 1996)

Abstract. The pyrolysis of 3-picoline dilute in argon was investigated using a single-pulse shock tube over the temperature range of 1400–1650 K and total pressures of 12–13 atm. The principal products observed were HCN, acetylene, benzene, cyanoacetylene, methane, and pyridine. Assuming that 3-picoline decomposes according to first-order kinetics, the rate constant for its overall disappearance was determined to be $k_{dis} = 10^{16.9\,(\pm 0.8)} \exp[-99\ (\pm 6)\ \text{kcal mol}^{-1}/RT]\ \text{s}^{-1}$. The principal initial decomposition routes were found to be via the formation of the 3-picolyl and *m*-pyridyl radicals whose subsequent ring-opening led to the observed products. A 68-step kinetic model was developed that successfully fits the experimental data. The dominant reactions, i.e., the formation of picolyl and pyridyl radicals and their subsequent chain-opening reactions, were studied using ab initio quantum chemical techniques. The ab initio data were also incorporated into the kinetic model in the form of energies and A-factors for reactions for which no kinetic or thermochemical data were previously available. Optimization of the kinetic model yields a value of $64 \pm (3)$ kcal mol^{-1} for the heat of formation of 3-picolyl, a value lower than that for 2-picolyl, suggesting that the decomposition of 3-picoline more closely resembles that of toluene, rather than its isomer 2-picoline.

INTRODUCTION

3-Picoline is one of the nitrogen-containing analogues of toluene, a compound much studied in terms of its combustion and pyrolysis. There have been many shock tube studies[1–5]conducted on toluene in an attempt to elucidate its mechanism of decomposition under conditions of high temperature and pressure.

Toluene may initially decompose via two possible pathways:

$$C_7H_8 \rightarrow C_7H_7 + H \qquad (a)$$

producing benzyl radicals, and

$$C_7H_8 \rightarrow C_6H_5 + CH_3 \qquad (b)$$

producing methyl and phenyl radicals. Thermochemistry suggests that pathway (a) is likely to be the more important, due to resonance stabilization of the benzyl radical, resulting in a lower activation energy for this reaction than for reaction (b). However, it was found that benzyl and H atoms recombine at a very rapid rate; consequently pathway (b) is more significant for product formation than first thought,[6] especially at higher temperatures. Moreover, there is some uncertainty with regard to the mechanism of the subsequent decomposition of benzyl radicals

$$C_7H_7 \rightarrow \text{benzyl fragments} + H \qquad (c)$$

(where the benzyl fragments may contain C_2H_2, C_3H_3, C_4H_4, and C_5H_5 molecules[7]), although there is now agreement as to the rate of (c).

Studies of the mechanisms of decomposition of N-analogues of toluene, viz., 2-, 3-, and 4-picoline, may provide us with additional information about the decomposition of toluene. Doughty et al.[8] carried out shock tube and kinetic modeling studies of the decomposition of 2-picoline and suggested that it may decompose in a way analogous to toluene:

$$C_6H_7N \rightarrow C_6H_6N + H \qquad (d)$$

forming the 2-picolyl radical (analogous to benzyl), and

$$C_6H_7N \rightarrow C_5H_4N + CH_3 \qquad (e)$$

forming the methyl and *o*-pyridyl radicals. Kinetic mod-

*Author to whom correspondence should be addressed.

eling supported the notion that both picolyl and pyridyl radicals subsequently underwent ring-opening and decomposition reactions into the observed products: HCN, acetylene, acetonitrile, acrylonitrile, cyanoacetylene, cyanocyclopentadiene, cyanovinylacetylene, and methane. The nitrogen atom in the ring serves as a useful chemical marker in determining the relative importance of each route and it was possible to discriminate between the products that had formed from the picolyl (d) and pyridyl (e) pathways. For toluene there has been some ambiguity as to whether the observed products arise from the reactions of benzyl or phenyl.

Doughty et al. found that routes (d) and (e) are both significant in determining the decomposition of 2-picoline, their relative importance changing with temperature. Abstraction reactions involving H, CH_3, and C_2H_3 radicals were also found to be important. The products HCN, 1-cyanocyclopentadiene, and cyclopentadiene were found to arise through the 2-picolyl pathway, while the products cyanoacetylene, methane, and acetylene were formed through the *o*-pyridyl + methyl route.

3-Picoline is expected to undergo a decomposition reaction similar to that of 2-picoline although the dominant pathway may be different, depending on the relative stabilities of the 3-picolyl and *m*-pyridyl radicals and the products formed when these radicals undergo ring opening. As there is little known about the thermochemistry of some of the radicals that are important in these decomposition processes, an ab initio study has been carried out to investigate the energetics of the key reactions. These have been incorporated into the kinetic model presented in this paper.

The present shock tube study of the pyrolysis of 3-picoline is also relevant to studies of the evolution of oxides of nitrogen (NO_x) from the combustion of coal. Much of the nitrogen contained in coal is in the form of pyridine and pyrrole ring structures[9] and 3-picoline, being one of the simplest substituted pyridines, may therefore be a useful model for reactions of coal bound nitrogen. The mechanism of formation of NO_x precursors, such as HCN, is therefore of importance in this case.

EXPERIMENTAL

A single-pulse shock tube (SPST) with i.d. of 7.6 cm was employed in this study. Analyses of the heavier hydrocarbons and nitrogen-containing species were carried out using a Hewlett-Packard HP5890/2 GC equipped with an FID and an NPD and light hydrocarbons were analyzed using a Shimadzu GC-9A using FID. Product identification was achieved using a Hewlett-Packard 5890/2 GC in conjunction with a Hewlett-Packard 5989 MS.

3-Picoline (Aldrich 99.5%) was further purified using three bulb-to-bulb distillations after degassing. Mixtures of 3-picoline in argon were prepared at concentrations of approximately 0.2 mol%. Pressures and temperatures behind the reflected shock were determined from the measured incident and reflected shock velocities. Pressures ranged from 12 to 13 atm, temperatures from 1400 to 1650 K, and residence times were between 650 and 900 μs.

COMPUTATIONAL

Ab initio quantum chemical methods were utilized in this study to obtain thermochemical data on the important radicals involved in the proposed decomposition scheme. All geometries were initially optimized using restricted Hartree–Fock (RHF) theory in conjunction with the 3-21G basis sets of Binkley et al.[10] The geometries of the open chain radicals resulting from the ring-opening reactions of pyridyl and picolyl, as well as of the associated transition-state structures, were obtained using multiconfigurational SCF calculations and 3-21G basis sets. The method of choice is the complete active space SCF (CASSCF) technique of Roos et al.,[11] with 9 active electrons (that includes all π-electrons) in 9 active orbitals. The harmonic frequencies were computed at the appropriate SCF or CASSCF levels of theory. Single point energy calculations were carried out at correlated levels of theory, namely (single configuration) second-order Møller–Plessett (MP2 or ROMP2) or multiconfiguration second-order perturbation theory (CASPT2),[12] using double zeta plus polarization functions (DZP)[13] or correlation consistent cc-pVDZ bases.[14] In the CASPT2 calculations the number of active electrons is 3, in an active space of 3 orbitals.

Test calculations have shown that the 3-21G basis is adequate for geometry optimizations, e.g., resulting in an energy difference of ~1 kcal mol^{-1} in comparison with the DZP optimized geometry in the case of the transition state of the ring-opening reaction of pyridyl. The adequacy of MP2/DZP calculations to predict the energetics of C–H bond-breaking reactions was tested in previous work of ours,[13] concluding that the calculated bond energies were accurate to within ca. 5%. Similar absolute accuracy may be expected for C–C bond-breaking reactions too.

The calculations were performed using the CADPAC,[15] SIRIUS,[16] ABACUS,[17] and MOLCAS2[18] programs on DEC alpha and IBM RS6000 workstations.

RESULTS AND DISCUSSION

3-Picoline was found to start decomposing at temperatures of ~1400 K. Its decomposition profile is shown in Fig. 1. The principal hydrocarbon products are acetylene and methane, and the principal nitrogen-containing products are HCN, cyanoacetylene, and pyridine. Profiles of the major products are shown in Figs. 2–4. The minor products are benzene, diacetylene, cyclopentadiene, ethane, ethylene, propyne, and vinyl acetylene. In addition, traces of 2-picoline, benzonitrile, cyanodiacetylene, cyanovinylacetylene, phenylethylene, and styrene were observed.

3-Picoline appears to undergo first-order decomposition kinetics. Although the range of concentrations studied was not large enough to rule out higher-order kinetics, subsequent kinetic modeling lent support to the assumption of first-order decomposition. An Arrhenius plot of the first-order rate constant for disappearance of 3-picoline between 1.5 and 50% decomposition yields the rate parameters $A_{dis} = 10^{16.9 \pm 0.8}$ s^{-1} and $E_{a,dis} = 99 \pm 6$ kcal mol^{-1}.

The results obtained from the theoretical ab initio calculations are shown in Table 1 as reaction and critical energies at 0 K, including zero point vibrational corrections. The thermal corrections to the absolute energies of the various species that are needed to calculate the reaction energies at 300 K are ~5 kcal mol^{-1}, but in the calculation of reaction energies these corrections largely cancel. For example, for the chain-opening reactions the thermal corrections to the energies quoted in Table 1 are ≤1 kcal mol^{-1}. The errors due to approximations in the level of correlation treatment and basis set are more significant, estimated as ~5 kcal mol^{-1} in the energies quoted. The energies that are in the kinetic model (to be discussed later) are also quoted in Table 1 for comparison with the ab initio values. The two sets of results are clearly consistent.

The ab initio energies in Table 1 were used as initial values for the activation energies in the kinetic model in Table 2. These values were then optimized (within the expected uncertainties of the calculations) to fit the experimental data. Similarly, the Arrhenius pre-exponential factors for reactions 9 and 19 in the kinetic model (Table 2) were estimated on the basis of the quantum chemical results for the transition states in these reactions, viz., using the predicted geometries to calculate the entropies of activation.

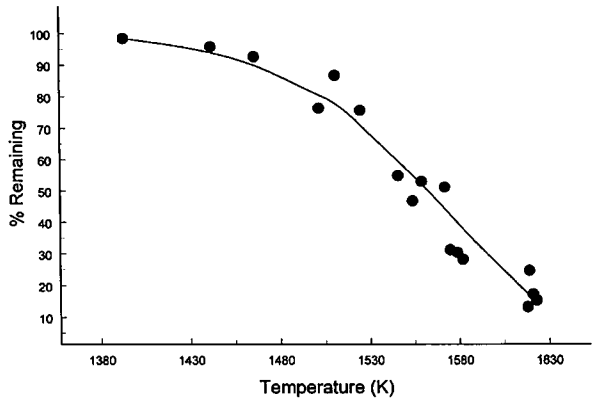

Fig. 1. Comparison of the experimental percentage of 3-picoline remaining (points) with the model prediction of Table 2 (line).

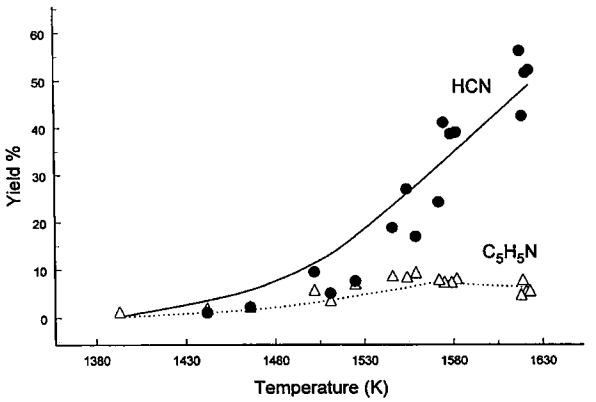

Fig. 3. Comparison of the experimental yield of HCN/pyridine (points/triangles) with the model prediction of Table 2 (line/dotted line).

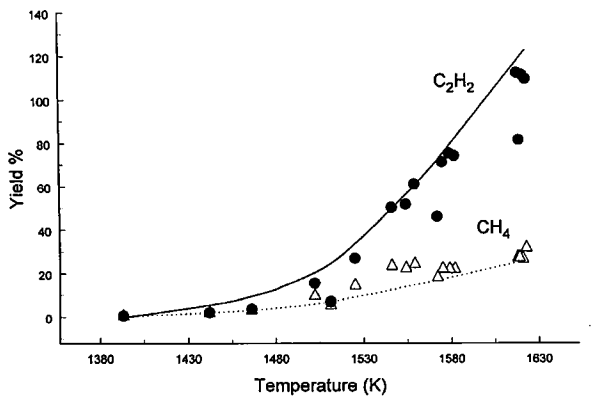

Fig. 2. Comparison of the experimental yield of acetylene/methane (points/triangles) with the model prediction of Table 2 (line/dotted line).

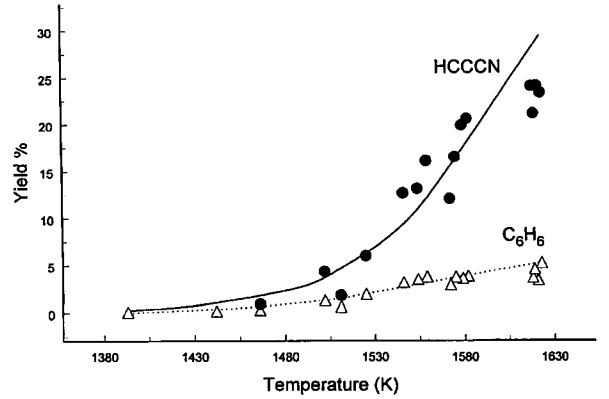

Fig. 4. Comparison of the experimental yield of cyanoacetylene/benzene (points/triangles) with the model prediction of Table 2 (line/dotted line).

Table 1. Ab initio energies (kcal mol^{-1}) of some key radicals and transition states (TS) in the decomposition process of 3-picoline and comparison with analogous values in the kinetic model

Molecule	Formula	Calculation	Energy	
			calculated	model
3-picolyl	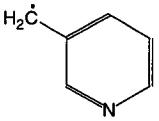	MP2/DZP// SCF/3-21G	88.2[a]	91.0[a]
m-pyridyl	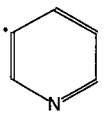	MP2/DZP// SCF/3-21G	104.2[b]	99.5[b]
o-pyridyl	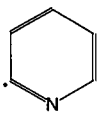	MP2/DZP// SCF/3-21G	98.4[b]	
L-[C_6H_6N]I	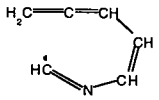	CASPT2/cc-pVDZ// CASSCF/3-21G	75.7[c,d] (71.3)[c,d]	74.0[c]
L-[C_6H_6N]I/TS	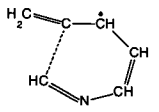	CASPT2/cc-pVDZ// CASSCF/3-21G	78.6[c,d] (75.3)[c,d]	78.0[c]
B-[C_4H_4CN]	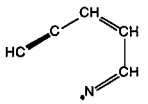	CASPT2/cc-pVDZ// CASSCF/3-21G	35.1[d,e] (31.8)[d,e]	29.7[e]
B-[C_4H_4CN]/TS	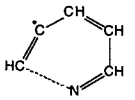	CASPT2/cc-pVDZ// CASSCF/3-21G	44.4[d,e] (43.0)[d,e]	43.0[e]
C_4H_4CN	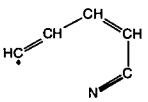	CASPT2/cc-pVDZ// CASSCF/3-21G	34.2[e,f] (30.7)[e,f]	31.4[f]
C_4H_4CN/TS	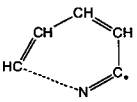	CASPT2/cc-pVDZ// CASSCF/3-21G	40.1[e,f] (37.8)[e,f]	40.0[f]

[a] relative to E(3-picoline)–E(H).
[b] relative to E(3-picoline)–E(CH_3).
[c] relative to E(3-picolyl).
[d] CASPT2 energies using diagonal and (non-diagonal) representation of zeroth order Hamiltonian.
[e] relative to E(*m*-pyridyl).
[f] relative to E(*o*-pyridyl).

In summary, initial decomposition of 3-picoline proceeds via two parallel initiation routes:

$$\text{3-picoline} \rightarrow \text{3-picolyl} + \text{H} \quad (1)$$

$$\text{3-picoline} \rightarrow m\text{-pyridyl} + \text{CH}_3 \quad (2)$$

Fission of the methyl side chain to form the *m*-pyridyl radical in reaction 2 is 15 kcal mol^{-1} more energetic than loss of H to form 3-picolyl. This result contrasts with that found previously for 2-picoline,[8] where the route to *o*-pyridyl had the lower activation energy. In the present case we expect that a greater proportion of the observed products arise from route 1. This situation is more akin to toluene, where the main decomposition pathway is via the benzyl radical,[4] as discussed in more detail below.

Braun-Unkoff et al.[2] proposed that benzyl could rearrange and undergo decomposition via a norbornadienyl intermediate. This was postulated to explain their low observed activation energy (44.7 kcal mol^{-1}) for the reaction

$$\text{C}_7\text{H}_7 \text{ (benzyl)} \rightarrow \text{C}_5\text{H}_5 \text{ (cyclopentadienyl)} + \text{C}_2\text{H}_2$$

They discounted the formation of a linear C_5H_5 radical on the grounds of the large activation energy that had been expected for the simple ring fission of benzyl.

Doughty et al.[8] considered an analogous route to the above in the case of 2-picoline to explain the formation of 1-cyanocyclopentadiene and the cyclopentadienyl radical. It was rejected, since the expected products of this route, viz., pyrrole, substituted pyrroles, and their corresponding decomposition products, were not observed experimentally. A decomposition route via a seven-membered ring was rejected on similar grounds.

The mechanism that best describes the decomposition of 2-picoline is one involving direct ring opening of both *o*-pyridyl and 2-picolyl. Although the direct ring fission has high activation energies, Doughty et al.[8] nevertheless showed it to be a feasible process over the temperature range studied.

The possibility that 3-picoline may decompose by direct ring-opening pathways was therefore seriously considered. The expected products of ring-opening reactions of both 3-picolyl and *m*-pyridyl are open-chain radicals whose heats of formation are higher than their counterparts for 2-picoline. However, our ab initio calculations (Table 1) indicate that these barriers are ~78 kcal mol^{-1} for 3-picolyl and only ~44 kcal mol^{-1} for *m*-pyridyl, supporting the hypothesis that these ring-opening reactions are viable decomposition pathways at the temperature range of this study. We have discounted decomposition via a norbornadienyl-like intermediate or a seven-membered ring because these routes would give rise to products not observed experimentally (as was the case with 2-picoline). A brief description of the possible products formed from the ring-opening mechanisms for 3-picoline follows.

The most likely fate of the L-C_6H_6NI radical formed by the ring opening of 3-picolyl (reaction 9) is decomposition into HCN and the open chain A-C_5H_5 radical (reaction 10). (See Table 1 for the labeling of these and other radicals referred to below.) The linear C_5H_5 radical may then either fission into propargyl and acetylene (reaction 11) or undergo cyclization to form the cyclopentadienyl radical (reaction 12), as in the 2-picoline decomposition scheme.[8] Propargyl may then form benzene or propyne, both of which are observed among the decomposition products.

The product of the ring-opening reaction of *m*-pyridyl, B-C_4H_4CN, may either directly decompose into HCN and *n*-C_4H_3 or undergo a facile 1,4 H shift to form the C_4H_4CN radical, which is also the product of *o*-pyridyl ring opening. This is expected to proceed with a low barrier and is not rate determining. The C_4H_4CN radical decomposes according to the pyridine scheme,[8,19] giving rise to a range of products including cyanoacetylene.

The decomposition products of 3-picoline, viz., HCN, acetylene, benzene, propyne, cyanoacetylene, vinyl acetylene, and cyclopentadiene, may therefore be explained by the ring-opening schemes proposed above. Other products, such as pyridine, methane, ethane, and ethylene, arise primarily through abstraction or displacement reactions. Abstraction of a ring hydrogen from 3-picoline to form a methylpyridyl radical (*o*-CH_3PYR) is included in the model to account for the extra propyne and cyanoacetylene observed in the system.

By way of comparison, the analogous ring-opening reaction of the benzyl radical was also studied using the same theoretical methods as in the case of the 3-picolyl and pyridyl radicals. In stark contrast with 3-picolyl, the critical energy of the ring-opening reaction of the benzyl radical was calculated to be ~ 93 kcal mol^{-1}, i.e., ~ 20 kcal mol^{-1} higher than for 3-picolyl. Clearly, this pathway is energetically much too unfavorable in the case of the benzyl radical.

KINETIC MODELING

A 68-step model was developed to explain the decomposition of 3-picoline, as summarized in Table 2. As noted above, the thermochemical parameters for certain reactions were obtained from ab initio quantum chemical calculations, the results of which are given in Table

1. Other parameters were taken from references as shown.

The kinetic equations were integrated using the CHEMKIN package,[20] LSODE,[21] and the SANDIA[22] shock tube code, modified to take into account cooling effects by the reflected rarefaction wave. The SENKIN[23] code was used for rate of production and sensitivity analyses.

In Figs. 1–4, the experimental product and decomposition profiles are compared with those predicted by the model. The predicted profiles for the major products lie within the range of experimental error. The minor products (not shown) can also be predicted in reasonable agreement with experiment.

The sensitivity data shown in Fig. 5 demonstrate the near equal rate of disappearance of 3-picoline through

Table 2. Reaction model for 3-picoline pyrolysis[a]

	Reaction	Forward reaction			Reverse reaction			Ref
		log *A*	*n*	*E*	log *A*	*n*	*E*	
1	3-picoline ⇔ H + 3-picolyl	15.0	0	91.0	13.7	0	0.4	PW
2	3-picoline ⇔ *m*-pyridyl + CH_3	16.0	0	99.5	12.6	0	2.4	PW
3	CH_3 + 3-picoline ⇔ CH_4 + 3-picolyl	11.9	0	4.0	12.7	0	18.5	PW
4	H + 3-picoline ⇔ H_2 + 3-picolyl	13.0	0	3.2	12.3	0	17.1	PW
5	C_2H_3 + 3-picoline ⇔ C_2H_4 + 3-picolyl	13.0	0	1.5	14.2	0	16.5	PW
6	n-C_4H_3 + 3-picoline ⇔ C_4H_4 + 3-picolyl	12.9	0	2.5	13.7	0	19.5	PW
7	3-picoline + CH_3 ⇔ *o*-CH_3PYR + CH_4	12.3	0	12.0	12.5	0	9.2	PW
8	3-picoline + H ⇔ *o*-CH_3PYR + H_2	13.0	0	9.0	11.8	0	5.7	PW
9	3-picolyl ⇔ L-C_6H_6NI	15.7	0	78.0	11.7	0	4.0	QC
10	A-C_5H_5 + HCN ⇔ L-C_6H_6NI	11.9	0	5.0	13.6	0	7.0	8
11	A-C_5H_5 ⇔ C_3H_3 + C_2H_2	12.0	0	27.0	11.4	0	9.0	8
12	A-C_5H_5 ⇔ c-C_5H_5	11.6	0	25.0	16.3	0	80.0	PW
13	c-C_5H_5 + H ⇔ c-C_5H_6	14.9	0	0.0	15.4	0	78.9	8
14	*o*-CH_3PYR ⇔ B-C_6H_6N	14.7	0	33.0	10.6	0	8.5	est
15	B-C_6H_6N ⇔ C_3H_4P + HCCHCN	14.3	0	35.0	12.3	0	5.0	est
16	*m*-pyridyl + 3-picoline ⇔ pyridine + 3-picolyl	12.3	0	8.0	12.8	0	26.8	PW
17	*m*-pyridyl + CH_4 ⇔ pyridine + CH_3	12.3	0	4.0	12.0	0	8.3	est
18	*m*-pyridyl + H_2 ⇔ pyridine + H	12.9	0	3.2	14.1	0	8.1	est
19	*m*-pyridyl ⇔ B-C_4H_4CN	15.0	0	43.0	12.3	0	13.3	QC
20	B-C_4H_4CN ⇔ C_4H_4CN	12.0	0	15.4	13.0	0	18.0	QC
21	B-C_4H_4CN ⇔ HCN + n-C_4H_3	13.7	0	43.5	11.0	0	4.9	8
22	3-picoline + H ⇔ pyridine + CH_3	13.9	0	8.5	12.3	0	20.8	PW
23	pyridine ⇔ *o*-pyridyl + H	15.9	0	102.0	14.1	0	0.2	19
24	pyridine + H ⇔ *o*-pyridyl + H_2	13.5	0	5.0	12.3	0	7.7	19
25	pyridine + CH_3 ⇔ *o*-pyridyl + CH_4	12.0	0	4.0	12.3	0	7.3	8
26	2-picoline ⇔ *o*-pyridyl + CH_3	16.1	0	91.5	12.7	0	0.5	8
27	*o*-pyridyl ⇔ C_4H_4CN	14.0	0	40.0	11.7	0	8.6	19
28	C_4H_4CN ⇔ C_2H_2 + HCCHCN	13.2	0	37.0	10.9	0	2.8	19
29	C_4H_4CN ⇔ A-C_4H_4CN	13.0	0	18.0	12.1	0	23.9	8
30	HCCCN + C_2H_3 ⇔ A-C_4H_4CN	13.0	0	2.0	13.8	0	40.6	8
31	HCCHCN ⇔ HCCCN + H	12.0	0	41.0	12.8	0	2.1	8
32	H + HCCHCN ⇔ H_2CCHCN	13.3	0	0.0	15.2	0	105.6	8
33	H + H_2CCHCN ⇔ HCN + C_2H_3	13.0	0	4.0	11.1	0	4.4	19
34	H + H_2CCHCN ⇔ HCCHCN + H_2	13.7	0	8.0	12.5	0	6.9	8
35	H_2CCHCN + M ⇔ HCCCN + H_2 + M	16.7	0	80.0	16.3	0	40.0	8
36	2 (3-picolyl) ⇔ 3,3-dipicolyl	12.3	0	0.0	14.3	0	65.3	8
37	C_4H_4 ⇔ $2C_2H_2$	15.0	0	81.1	13.6	0	44.6	26
38	C_4H_4 ⇔ C_4H_2 + H_2	14.6	0	86.0	13.6	0	44.4	26
39	n-C_4H_3 ⇔ C_4H_2 + H	12.5	0	44.0	12.9	0	5.5	19
40	$2C_2H_5$ ⇔ C_2H_4 + C_2H_6	12.1	0	0.0	12.7	0	60.5	27
41	C_2H_5 (+ M) ⇔ C_2H_4 + H (+ M)	13.3	0	39.7	12.5	0	2.1	28
42	C_2H_4 + M ⇔ C_2H_2 + H_2 + M	17.4	0	79.3	15.9	0	37.8	28
43	C_2H_4 + M ⇔ C_2H_3 + H + M	17.4	0	96.6	15.0	0	-9.0	8

Table 2 *continued*

	Reaction	Forward reaction log *A*	*n*	*E*	Reverse reaction log *A*	*n*	*E*	Ref
44	$C_2H_4 + H \Leftrightarrow C_2H_3 + H_2$	13.7	0	8.0	11.9	0	6.9	29
45	$H + C_2H_2 (+ M) \Leftrightarrow C_2H_3 (+ M)$	13.0	0	2.7	12.7	0	43.1	30
46	$2CH_3 (+ M) \Leftrightarrow C_2H_6 (+ M)$	13.6	0	0.0	16.8	0	87.0	27
47	$2CH_3 \Leftrightarrow C_2H_4 + H_2$	16.0	0	32.0	17.8	0	87.9	28
48	$C_2H_6 + H \Leftrightarrow C_2H_5 + H_2$	2.7	3.5	5.2	14.6	0	22.2	31
49	$C_2H_6 + CH_3 \Leftrightarrow C_2H_5 + CH_4$	–6.82	6.0	6.1	15.6	0	31.2	27
50	$C_2H_2 + HCN \Leftrightarrow H_2CCHCN$	13.5	0	40.0	15.1	0	80.0	19
51	$CH_3 + H_2 \Leftrightarrow CH_4 + H$	2.8	3.0	7.7	15.1	0	17.3	31
52	$2C_3H_3 \Leftrightarrow C_4H_4 + C_2H_2$	12.5	0	0.0	13.5	0	38.3	31
53	$2C_3H_3 \Leftrightarrow$ L-C_6H_6	12.0	0	0.0	14.3	0	57.8	PW/31
54	L-$C_6H_6 \Leftrightarrow C_6H_6$	11.9	0	33.0	16.7	0	116.0	PW/31
55	$CN + H_2 \Leftrightarrow HCN + H$	5.7	2.44	2.1	15.0	0	27.4	32
56	$CN + C_2H_2 \Leftrightarrow C_2H + HCN$	12.7	0	3.0	12.5	0	0.6	19
57	$C_2H + HCN \Leftrightarrow HCCCN + H$	13.0	0	0.0	14.9	0	20.2	19
58	$CH_3 + C_2H_2 \Leftrightarrow C_3H_4P + H$	12.9	0	17.0	15.1	0	7.9	33
59	$C_3H_3 + H \Leftrightarrow C_3H_4P$	12.9	0	0.0	15.5	0	89.1	31
60	*n*-$C_4H_3 \Leftrightarrow C_2H_2 + C_2H$	14.5	0	57.0	13.8	0	3.4	34
61	$C_2H + H_2 \Leftrightarrow C_2H_2 + H$	12.9	0	0.0	13.6	0	20.3	35
62	$C_2H + C_2H_2 \Leftrightarrow C_4H_2 + H$	12.9	0	0.0	14.0	0	15.1	36
63	$C_2H + C_4H_2 \Leftrightarrow C_6H_2 + H$	12.7	0	0.0	14.0	0	14.8	19
64	*n*-$C_4H_3 + C_2H_2 \Leftrightarrow$ L-C_6H_5	12.0	0	3.0	14.2	0	38.7	34
65	L-$C_6H_5 \Leftrightarrow C_6H_5$	10.3	0	1.4	13.7	0	65.2	34
66	$C_6H_6 \Leftrightarrow C_6H_5 + H$	15.7	0	107.9	13.1	0	-2.8	37
67	$C_2H_3 + C_4H_2 \Leftrightarrow$ L-C_6H_5	12.0	0	3.0	14.1	0	36.8	34
68	$C_6H_6 + H \Leftrightarrow C_6H_5 + H_2$	14.4	0	16.0	12.4	0	9.8	38

[a] Units for *A*, $cm^3\ mol^{-1}\ s^{-1}$ or s^{-1} as appropriate. Units for *E*, kcal mol^{-1}. PW indicates rate constant evaluated in the present work; est indicates rate constant estimated in the present work; QC indicates rate constant estimated by ab initio techniques in the present work.

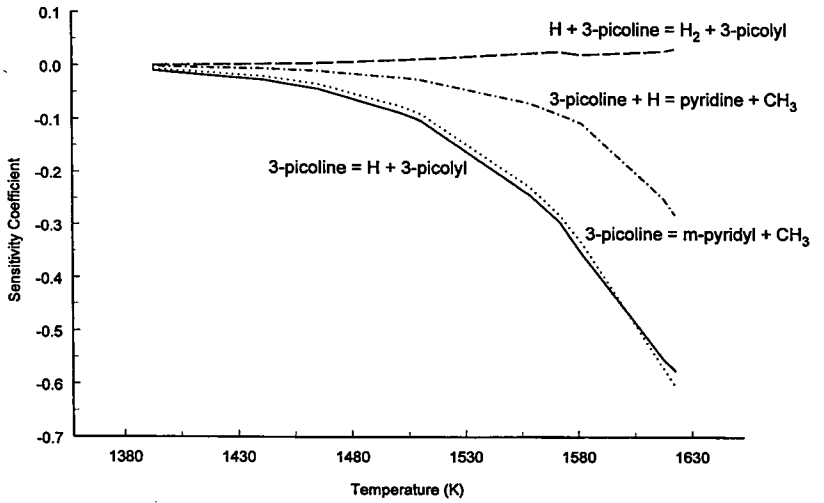

Fig. 5. Temperature variation of the sensitivity coefficients for 3-picoline.

reaction channels 1 and 2. While reaction 1 is slightly more sensitive at lower temperatures, reaction 2 is more important at higher temperatures, although neither is dominant. This is in contrast with 2-picoline, where it was found that the *o*-pyridyl route is significantly more important at all temperatures.[8] This is consistent with 3-picolyl being more stable than 2-picolyl, as well as with the lower stability of *m*-pyridyl in comparison with *o*-pyridyl. In 3-picoline the picolyl decomposition pathway is relatively more important than in 2-picoline. Thus, the decomposition of 3-picoline resembles that of toluene more than that of 2-picoline. It should be

pointed out, however, that rate of production analysis reveals that only 27–30% of the 3-picoline actually decomposes via reaction 1. This is because reaction 1 readily equilibrates, whereas reaction 2 is essentially irreversible under the conditions of our experiments.

Our rate expressions for reactions 1 and 2 of Table 2 may be compared with the analogous expressions for decomposition of toluene where $A = 10^{15.0}$ s^{-1} and E_a = 86.1 kcal mol^{-1} for production of benzyl + H[24], and $A = 10^{16.1}$ s^{-1} and E_a = 94.4 kcal mol^{-1} for the channel to phenyl + CH_3[3]. A-factors are seen to be quite similar for the two decomposition channels of 3-picoline and toluene, whereas the activation energies for 3-picoline channels are 5 kcal mol^{-1} higher in both cases.

Sensitivity and rate of production analyses indicate that the major products HCN and acetylene (refer to Figs. 6 and 7), as well as the minor product benzene, are formed primarily through the 3-picolyl decomposition pathway. The *m*-pyridyl pathway accounts for much of cyanoacetylene formed, while methane and pyridine mainly arise through the abstraction and displacement reactions 2 and 22, respectively. The rate-determining step for the disappearance of 3-picolyl via ring fission is reaction 9, and Arrhenius parameters obtained from the ab initio calculations are $A = 10^{15.7}$ s^{-1} and E_a = 78.0 kcal mol^{-1}. The corresponding experimental values for the disappearance of benzyl[24] are $A = 10^{15.3}$ s^{-1} and E_a = 83.7 kcal mol^{-1}, although there is uncertainty about the products of decomposition. Our ab initio calculations of the barrier to ring opening (~ 93 kcal mol^{-1}) are much larger than the experimental value, thus the possibility of direct ring opening is effectively eliminated.

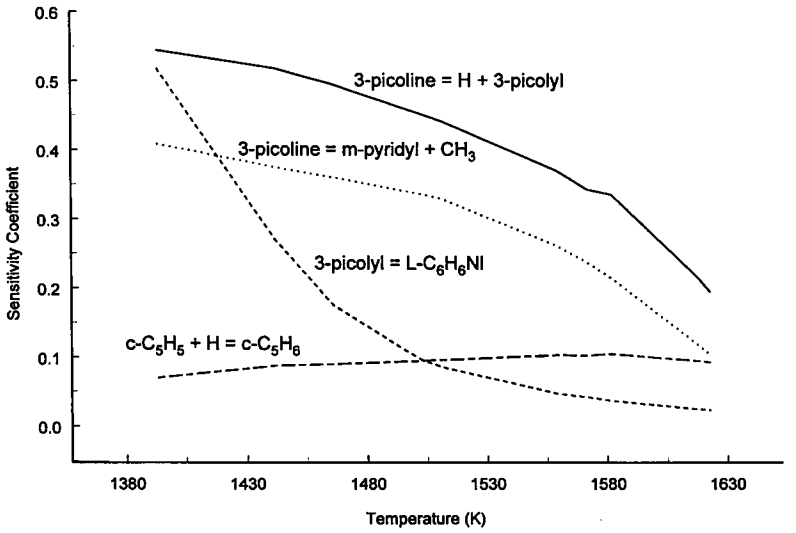

Fig. 6. Temperature variation of the sensitivity coefficients for HCN.

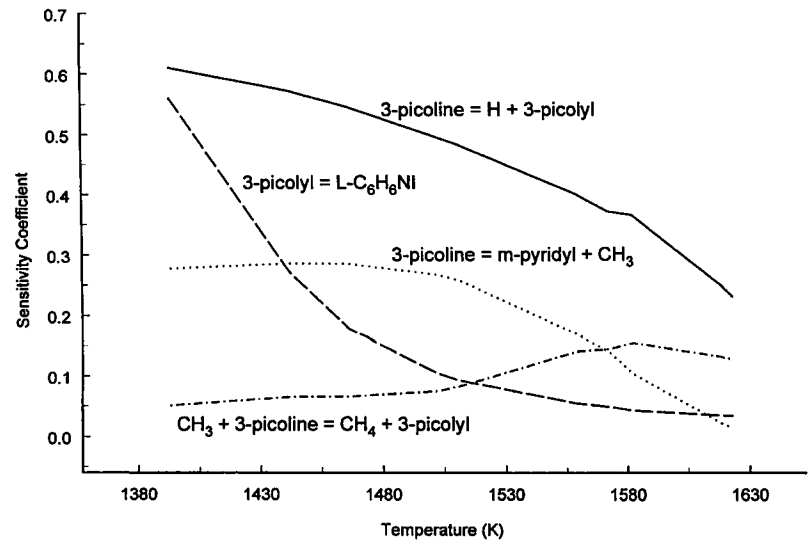

Fig. 7. Temperature variation of the sensitivity coefficients for acetylene.

The model exhibits a moderate degree of sensitivity to reaction 1, so that the Arrhenius parameters for this reaction can be used to determine an approximate value for the heat of formation of the 3-picolyl radical. A value of 64 ± (3) kcal mol^{-1} at 300 K is obtained this way, which is ~ 4 kcal mol^{-1} below the heat of formation of 2-picolyl, possibly due to a greater degree of resonance stabilization in the former. In the case of benzyl, its recombination with H was found[6] to have an anomalously high rate constant of 2.5×10^{14} cm^3 mol^{-1} s^{-1}, this value being attributed to the resonance stability of the benzyl radical. However, our rate constant for the analogous reaction, i.e., recombination of 3-picolyl with H was found to be 5×10^{13} cm^3 mol^{-1} s^{-1}, i.e., within the "normal" range, suggesting a lower degree of resonance than in benzyl.

It has been found that in toluene pyrolysis the production of stilbene is an important factor in accounting for the disappearance of benzyl radicals.[24,25] The mechanism of stilbene formation involves the recombination of two benzyl radicals to make dibenzyl initially, followed by loss of hydrogen to form stilbene. This process may be expected to take place in 3-picoline and would be initiated by the recombination of two 3-picolyl radicals to form 3,3-dipicolyl (included as reaction 36 in the model). However, 3,3-dipicolyl and its decomposition products were not observed in our experiments, so this pathway was not investigated further in the model. As noted, the rate constant for reaction 36 was chosen from the previous work on 2-picoline.[8]

As indicated previously, the decomposition of *m*-pyridyl proceeds in a manner similar to that of *o*-pyridyl,[8,19] hence a portion of this reaction mechanism appears in Table 2 as reactions 23–30. According to the ab initio calculations, the initial rearrangement from B-C_4H_4CN to C_4H_4CN is close to thermoneutral and proceeds with a pre-exponential factor of 10^{12} s^{-1} and barrier of about 15 kcal mol^{-1}.

The model is also fairly sensitive to reactions which abstract hydrogen from the methyl group of 3-picoline (reactions 3–6). In particular, 40% of the methane produced at 1560 K is from reaction 3.

CONCLUSIONS

The thermal decomposition of 3-picoline has been successfully modeled using a 68-step reaction scheme. The rate constants were chosen on the basis of previous work or were estimated using ab initio quantum chemical calculations. All major products are successfully predicted within experimental limits and minor products are also satisfactorily modeled.

We find that there are two possible initiation reactions of 3-picoline: loss of a hydrogen atom, producing 3-picolyl radicals, and loss of methyl, resulting in *m*-pyridyl radicals. Both of these species readily undergo ring-opening reactions to form the observed major products: HCN, acetylene, benzene, and cyanoacetylene. In addition, displacement reactions are important in the formation of methane and pyridine. The disappearance of 3-picoline was found to be marginally more sensitive to reaction 1 than 2 at temperatures less than 1600 K. In this respect, the decomposition of 3-picoline is quite similar to that of toluene.

REFERENCES AND NOTES

(1) Astholz, D.C.; Troe, J. *J. Chem. Soc., Faraday Trans. 2* **1982**, *78*, 1413–1421.

(2) Braun-Unkoff, M.; Frank, P.; Just, T. *22nd Symp. (Int.) on Combustion*; The Combustion Institute: Pittsburgh, 1988, pp 1053–1061.

(3) Pamidimukkala, K.M.; Kern, R.D.; Patel, M.R.; Wei, H. C.; Kiefer, J.H. *J. Phys. Chem.* **1987**, *9*, 2148–2154.

(4) Brouwer, L.D.; Müller-Markgraf, W.; Troe, J. *J. Phys. Chem.* **1988**, *92*, 4905–4914.

(5) Colket, M.B.; Seery, D.J. *25th Symp. (Int.) on Combustion*; The Combustion Institute: Pittsburgh 1994, pp 883–891.

(6) Ackermann, L.; Hippler, H.; Pagsberg, P.; Reihs, C.; Troe, J. *J. Phys. Chem.* **1990**, *94*, 5247–5251.

(7) Müller-Markgraf, W.; Troe, J. *J. Phys. Chem.* **1988**, *92*, 4899–4905.

(8) Doughty, A.; Mackie, J.C. *J. Phys. Chem.* **1990**, *96*, 10339–10348. (b) Terentis, A.; Doughty, A.; Mackie, J.C. *J. Phys. Chem.* **1990**, *96*, 10334–10339.

(9) Snyder, L.R. *Anal. Chem.* **1969**, *41*, 314–323.

(10) Binkley, J.S.; Pople, J.A.; Hehre, W.J. *J. Am. Chem. Soc.* **1980**, *102*, 939–947.

(11) Roos, B.O.; Taylor, P.R.; Siegbahn, P.E.M. *Chem. Phys.* **1980**, *48*, 157–173.

(12) Andersson, K.; Roos, B.O. *Int. J. Quantum Chem.* **1993**, *45*, 591–607.

(13) Jones, J.; Bacskay, G.B.; Mackie, J.C.; Doughty, A. *J. Chem. Soc., Faraday Trans.* **1995**, *91*, 1587–1592.

(14) Dunning, T.H. *J. Chem. Phys.* **1989**, *90*, 1007–1023.

(15) CADPAC 5.0: The Cambridge Analytical Derivatives Package Issue 5.0, Cambridge, 1992. A suite of quantum chemistry programs developed by Amos, R.D. with contributions from Alberts, I.L.; Andrews, J.S.; Calwell, S.M.; Handy, N.C.; Jayatilaka, D.; Knowles, P.J.; Kobayashi, R.; Koga, N.; Laidig, K.E.; Maslen, P.E.; Murray, C.W.; Rice, J.E.; Sanz, J.; Simandiras, E.D.; Stone, A.J.; Su, M.-D.

(16) Jensen, H.J.; Ågren, H.; Olsen, J. SIRIUS MCSCF program.

(17) Helgaker, T.; Jensen, H.J.; Jørgensen, P.; Olsen, J.; Taylor, P.R. ABACUS MCSCF energy derivatives program.

(18) Andersson, K.; Blomberg, M.R.A.; Fülscher, M.P.; Kellö, V.; Lindh, R.; Malmquist, P.-Å.; Noga, J.; Olsen, J.; Roos, B.O.; Sadlej, A.J.; Siegbahn, P.E.M.; Urban,

M.; Widmark, P.-O. MOLCAS version 2, University of Lund, Sweden, 1991.
(19) Mackie, J.C.; Colket, M.B.; Nelson, P.F. *J. Phys. Chem.* **1990**, *94*, 4099–4106.
(20) Kee, R.J.; Miller, J.A.; Jefferson, T.H. CHEMKIN: A General Purpose, Problem Independent, Transportable FORTRAN Chemical Kinetics Code Package. SANDIA National Laboratories Report SAND80-003, Mar. 1980.
(21) Hindmarsh, A.C. LSODE and LSODI; Two New Initial Value Differential Equation Solvers. *ACM Signem Newslett.* 1980, **15**: 4.
(22) Mitchell, R.E.; Kee, R.J. A General Purpose Computer Code for Predicting Chemical Kinetic Behavior behind Incident and Reflected Shocks. SANDIA National Laboratories Report SAND82-8205, Mar. 1982.
(23) Lutz, A.E.; Kee, R.J.; Miller, J.A. SENKIN: A FORTRAN Program Predicting Homogeneous Gas Phase Chemical Kinetics with Sensitivity Analysis. SANDIA National Laboratories Report SAND87-8248, Feb. 1988.
(24) Hippler, H.; Reihs, C.; Troe, J. *Z. Phys. Chem. N. F.* **1990**, *167*, 1–16.
(25) Frisch, S.; Hippler, H.; Troe, J. *Z. Phys. Chem.* **1995**, *188*, 259–273.
(26) Kiefer, J.H.; Mitchell, K.I.; Kern, R.D.; Yong, J.N. *J. Phys. Chem.* **1988**, *92*, 677–685.
(27) Baulch, D.L.; Cobos, C.J.; Cox, R.A.; Esser, C.; Frank, P.; Just, T.; Kerr, J.A.; Pilling, M.J.; Troe, J.; Walker, R.W.; Warnatz, J. *J. Phys. Chem. Ref. Data* **1992**, *21*, 411–429.
(28) Warnatz, J. *Combustion Chemistry*; Gardiner, W.C. Jr., Ed.; Springer-Verlag: New York, 1984, p 197.
(29) Weissman, M.A.; Benson, S.W. *J. Phys. Chem.* **1988**, *92*, 4080–4084.
(30) Payne, W.A.; Stief, L.J. *J. Chem. Phys.* **1976**, *64*, 1150–1155.
(31) Organ, P.P.; Mackie, J.C. *J. Chem. Soc., Faraday Trans.* **1991**, *87*, 815–823.
(32) Atakan, B.; Jacobs, A.; Wahl, M.; Weller, R.; Wolfrum, *J. Chem. Phys. Lett.* **1989**, *154*, 449–453.
(33) Hidaka, Y.; Nakamura, T.; Tanaka, H.; Inami, K.; Kawano, H. *Int. J. Chem. Kinet.* **1990**, *22*, 701–709.
(34) Colket, M.B. *21st Symp. (Int.) on Combustion*; The Combustion Institute: Pittsburgh 1986, pp 851–864.
(35) Kiefer, J.H.; Kapsalis, S.A.; Al-Alami, M.Z.; Budach, K.A. *Combust. Flame* **1983**, *51*, 79–93.
(36) Westmoreland, P.R. *Preprints ACS Div. Fuel Chem.* **1987**, *32*: 480–487.
(37) Hsu, D.S.Y.; Lin, C.Y.; Lin, M.C. *20th Symp. (Int.) on Combustion;* The Combustion Institute: Pittsburgh, 1984, pp 623–630.
(38) Kiefer, J.H.; Mizerka, L.J.; Patel, M.R.; Wei, H.-C. *J. Phys. Chem.* **1985**, *89*, 2013–2019.